Regulation of the desensitization and ion selectivity of ATP-gated $P2X_2$ channels by phosphoinositides

Yuichiro Fujiwara[1] and Yoshihiro Kubo[1,2,3]

[1] *Division of Biophysics and Neurobiology, Department of Molecular Physiology, National Institute for Physiological Sciences, Aichi 444-8585, Japan*
[2] *COE Program for Brain Integration and its Disorders, Tokyo Medical and Dental University Graduate School and Faculty of Medicine, Tokyo 113-8519, Japan*
[3] *SORST, Japan Science and Technology Corporation, Saitama 332-0012, Japan*

Phosphoinositides (PIP_ns) are known to regulate the activity of some ion channels. Here we determined that ATP-gated $P2X_2$ channels also are regulated by PIP_ns, and investigated the structural background and the unique features of this regulation. We initially used two-electrode voltage clamp to analyse the electrophysiological properties of $P2X_2$ channels expressed in *Xenopus* oocytes, and observed that preincubation with wortmannin or LY294002, two PI3K inhibitors, accelerated channel desensitization. K365Q or K369Q mutation of the conserved, positively charged, amino acid residues in the proximal region of the cytoplasmic C-terminal domain also accelerated desensitization, whereas a K365R or K369R mutation did not. We observed that the permeability of the channel to *N*-methyl-D-glucamine (NMDG) transiently increased and then decreased after ATP application, and that the speed of the decrease was accelerated by K365Q or K369Q mutation or PI3K inhibition. Using GST-tagged recombinant proteins spanning the proximal C-terminal region, we then analysed their binding of the $P2X_2$ cytoplasmic domain to anionic lipids using PIP_ns-coated nitrocellulose membranes. We found that the recombinant proteins that included the positively charged region bound to PIPs and PIP_2s, and that this binding was eliminated by the K365Q and K369Q mutations. We also used a fluorescence assay to confirm that fusion proteins comprising the proximal C-terminal region of $P2X_2$ with EGFP expressed in COS-7 cells closely associated with the membrane. Taken together, these results show that membrane-bound PIP_ns play a key role in maintaining channel activity and regulating pore dilation through electrostatic interaction with the proximal region of the $P2X_2$ cytoplasmic C-terminal domain.

(Resubmitted 9 June 2006; accepted after revision 14 July 2006; first published online 20 July 2006)
Corresponding authors Y. Fujiwara and Y. Kubo: Division of Biophysics and Neurobiology, Department of Molecular Physiology, National Institute for Physiological Sciences, Aichi 444-8585, Japan. Email: yuichiro@nips.ac.jp or ykubo@nips.ac.jp

Phosphoinositides (PIP_ns) are membrane lipids in the cytoplasmic leaflet of the plasma membrane, where they coexist with a variety of membrane proteins, including receptors and ion channels. The level of PIP_ns in the plasma membrane is dynamically modulated by phosphatases, kinases and phospholipases (Prestwich, 2004) (Fig. 1). For example, it is well known that phospholipase C (PLC) is activated by stimulation of G_q-coupled receptors and that it downregulates levels of $PI(4,5)P_2$ in the plasma membrane (Toker, 1998) (Fig. 1). In addition, signalling by Ras and tyrosine kinase growth factor receptor is known to activate phosphoinositide-3 kinase (PI3K), which catalyses the synthesis of 3-phosphorylated lipids ($PI(3)P_n$s) (Prestwich, 2004). These lipid signals play important roles in various aspects of cell biology, including endosome dynamics (Corvera, 2001), cell adhesion (Weiner *et al.* 2002), and oncogenesis (Vanhaesebroeck *et al.* 2001). In addition, PIP_ns also were recently shown to exert a modulatory effect on the activity of various ion channels (Hilgemann *et al.* 2001). For example, $PI(4,5)P_2$ directly activates the inward rectifier K^+ channel (Kir) (Baukrowitz *et al.* 1998; Huang *et al.* 1998; Shyng & Nichols, 1998; Liou *et al.* 1999), and insufficient interaction between $PI(4,5)P_2$ and Kir channels leads to Andersen's or Bartter's syndrome (Schulte *et al.* 1999; Lopes *et al.* 2002; Donaldson *et al.* 2003). PIP_ns also modulate the activity of the two-pore domain K^+ channels (Czirjak *et al.* 2001; Chemin *et al.* 2005), voltage-gated K^+ channels (Suh & Hille, 2002; Oliver *et al.* 2004), voltage-gated Ca^{2+} channels (Wu *et al.* 2002), transient receptor potential channels (Hardie *et al.* 2001), small-conductance Ca^{2+}-activated K^+ channels (Srivastava *et al.* 2005) and epithelial Na^+

 DOI: 10.1113/jphysiol.2006.115246

channels (Pochynyuk *et al.* 2005). However, regulation by PIP_ns had not been reported for the ATP receptor (P2X) channel.

P2X receptors are ligand-gated cation channels activated by extracellular ATP and are widely distributed in brain, peripheral nerves, smooth muscle and blood cells (Ralevic & Burnstock, 1998; North, 2002; Inoue *et al.* 2004). To determine the extent to which the $P2X_2$ channel is also regulated by PIP_ns, we initially analysed its electrophysiological properties, focusing on channel desensitization. The rate at which P2X family members desensitize varies (Ralevic & Burnstock, 1998; North, 2002): whereas $P2X_1$ and $P2X_3$ desensitize very rapidly, $P2X_2$, $P2X_5$ and $P2X_6$ do so only slowly. The desensitization of $P2X_4$ is intermediate, while that of $P2X_7$ is slow, and both of those channels show delayed increases in current amplitude (Surprenant *et al.* 1996; Khakh *et al.* 1999*a*). Desensitization of P2X is reportedly caused by time-dependent changes in the conformation of the transmembrane region of the channel after opening by ATP (Werner *et al.* 1996), and the cytoplasmic C-terminal domain of the channel appears to play a key role in determining the extent and rate of desensitization (Koshimizu *et al.* 1999; Smith *et al.* 1999). In spite of these works, it is not yet clear how these effects are mediated.

In addition to desensitization, the conformational changes after the channel opening are also observed in the dynamic changes in the ion selectivity of P2X channels, which occur within a time frame measured in seconds (Surprenant *et al.* 1996; Khakh *et al.* 1999*b*; Virginio *et al.* 1999). Whereas only small cations such as Na^+ and K^+ are able to pass through the channel pore immediately after ATP application, cations as large as *N*-methy-D-glucamine (NMDG) are able pass through the channel later (Virginio *et al.* 1999; Eickhorst *et al.* 2002; Fujiwara & Kubo, 2004), suggesting time-dependent expansion of the open pore. It would be of interest to know whether desensitization and pore dilation, both of which occur in a time-dependent manner after ATP application, are regulated by related mechanisms.

Focusing on the regulation of $P2X_2$ channel activity by PIP_ns, our aim in the present study was to use electrophysiological techniques to analyse desensitization and NMDG permeation of the channel. Within that context, we used mutagenesis as well as biochemical and the fluorescence analyses to examine the structural background of the interaction between $P2X_2$ and PIP_ns.

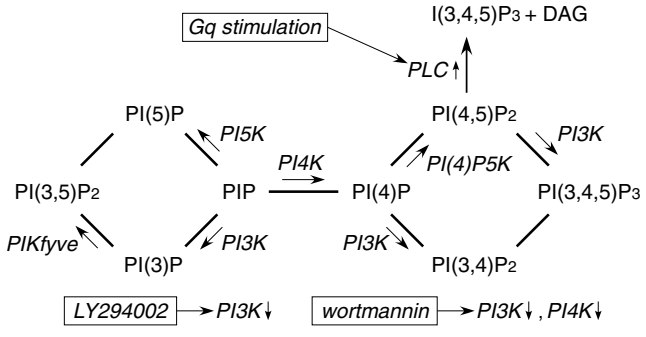

Figure 1. Metabolic map showing the relationships among various PIP_ns and PI-kinases
The sites of action of the indicated PI-kinases, kinase inhibitors and G_q-coupled receptor stimulation are indicated.

Methods

Molecular biology

A *Bam*H1–*Not*1 fragment of the original rat $P2X_2$ receptor cDNA (Brake *et al.* 1994) was subcloned into pBluescript vector. Single point mutations or a deletion mutation (S378stop) were introduced using a QuikChange site-directed mutagenesis kit (Stratagene), and confirmed by DNA sequencing. Double-point mutants were produced using single-point mutants as templates. cRNAs encoding the wild-type (WT) and mutant receptors were prepared from linearized plasmid cDNA using an RNA transcription kit (Stratagene). Glutathione-*s*-transferase (GST)-tagged constructs of the proximal C-terminal region of the $P2X_2$ channel (L353–S377) and its mutants were constructed using PCR with primers that included *Bam*HI(5′) and *Xho*I(3′) sites, after which the *Bam*HI-$P2X_2$(L353-S378stop)-*Xho*I fragments were subcloned into the pGEX-5X-1 vector (GE Healthcare Bio-Sciences). Constructs of fusion proteins encoding EGFP with various C-terminal fragments of the $P2X_2$ channel (L353–L472, L353–S378stop and S378–L472) were produced by inserting the *Bgl*II-$P2X_2$(C-terminus)-*Pst*I fragment into the EGFP-C1 vector (Clontech) in frame. DNA sequences of the inserted $P2X_2$ fragments and the regions surrounding the constructs were confirmed.

Electrophysiology

Xenopus oocytes were collected from frogs anaesthetized in water containing 0.15% tricaine, after which the frogs were killed by decapitation (Fujiwara & Kubo, 2002). The isolated oocytes were then treated with collagenase (2 mg ml^{-1}, type 1, Sigma), and those of similar size at stage V were injected with approximately 50 nl of cRNA solution (Fujiwara & Kubo, 2004), after which they were incubated for 2–3 days at 17°C in frog Ringer solution. All experiments conformed to the guidelines of the Animal Care Committees of National Institute for Physiological Sciences, JAPAN.

Macroscopic currents were recorded from the oocytes using the two-electrode voltage-clamp technique with a bath-clamp amplifier (OC-725C, Warner Co.).

Stimulation, data acquisition and data analysis were all done on a Pentium-based computer using Digidata 1322 A and pCLAMP 8.2 software (Axon Instruments). Intracellular glass microelectrodes were filled with 3 M potassium acetate with 10 mM KCl (pH 7.2). The microelectrode resistances ranged from 0.1 to 0.3 MΩ. Two Ag–AgCl pellets (Warner Co.) were used to pass the bath current and sense the bath voltage. The bath voltage-sensing pellet was placed near the oocyte (approximately 2 mm away) on the same side as the voltage-recording microelectrode. The bath current-passing pellet and the current injection microelectrode were placed on the other side.

Recordings were made at room temperature (20–23°C) in external bath solution containing 95.6 mM NaCl, 1 mM $MgCl_2$, 5 mM Hepes and 2.4 mM NaOH (pH 7.35–7.40). For the experiment on NMDG permeability summarized in Fig. 6, the bath solution contained 98 mM NMDG, 85 mM HCl, 1 mM $MgCl_2$ and 5 mM Hepes (pH 7.35–7.40). Ca^{2+} was excluded from the bath solution to avoid channel inactivation (Ding & Sachs, 2000) and a variety of secondary intracellular effects. Prior to recording, the bath was continuously perfused with external solution; however, perfusion of the bath was stopped once recording was begun. ATP disodium salt (SIGMA-Aldrich Co) was dissolved in bath solution just before each experiment, and the pH was adjusted to 7.35 using NaOH. When applied to cells, a one-fifth bath volume of five times concentrated ATP solution was pipetted into the bath, after which complete exchange of the solution around the oocyte was confirmed to occur within ∼0.5 s (Fujiwara & Kubo, 2004). Then after making the desired recordings, the ATP was washed out of the bath by perfusion with external solution without ATP.

The data in Figs 2–4 were recorded by applying a saturating concentration of ATP (100 μM) at a holding potential of −60 mV with the DC gain booster of the amplifier turned on. All of the PIP_n-disrupting regents were purchased from SIGMA-Aldrich Co, and were dissolved in DMSO. The oocytes were preincubated with the drugs before recordings were made; control oocytes were preincubated in the appropriate concentration of DMSO. In Fig. 4*C*, the ATP concentration–response relationships for the WT and mutant channels were analysed as follows. Oocytes injected with the same amount of cRNA were prepared, and the amplitudes of ATP-evoked currents were measured using two-electrode voltage clamp at −60 mV. To each oocyte, we applied one concentration of ATP one time; repeated application of ATP caused marked desensitization of the channel. The mean values of the response amplitudes to each concentration were plotted and fitted with Hill's equation, yielding a K_d value.

The reversal potentials in Fig. 6 were determined by applying 360 ms ramp pulses from −90 to 0 mV every 500 ms for 90 s after ATP application. We showed previously that the oocyte resting membrane potential (∼−30 mV) before the ATP application is mainly dependent on a small endogenous Cl^- conductance (Fujiwara & Kubo, 2004). In the present study, we obtained ATP-evoked $P2X_2$ channel currents by subtracting the data obtained before ATP application from those obtained after ATP application. This leaves the ATP-evoked currents (nominally) uncontaminated by other currents (e.g. leak current), so that reversal potentials obtained are those of the ATP-evoked current through the expressed $P2X_2$ channels. Actual clamped membrane potentials were monitored during current recordings, and data with an error of over 2 mV from the command potential were discarded.

The electrophysiological data were analysed using Clampfit (Axon Instruments, Inc.), Igor Pro (WaveMetrics, Inc) or KyPlot (Kyence Co.). The mean values of two groups were statistically compared using Student's *t* test (e.g. in Fig. 2*B*). The mean values of two groups among three or more groups were statistically compared using Tukey's test (e.g. comparison of means between WT and K365Q in Fig. 4*B*). Data from the same batch of oocytes were used for each set of analyses because properties such as channel desensitization and the permeability of large cations differed from batch to batch. Nevertheless, similar tendencies were reproducibly observed in three batches of oocytes in all experiments.

Biochemistry

Escherichia coli strain BL21-CodonPuls were transformed with GST-tagged WT or mutant plasmids and then cultured for 14 h at 25°C in 2YT medium supplemented with 20 μM isopropyl-thio-β-D-galactopyranoside and 0.1 mg ml^{-1} ampicillin, after which they were collected by centrifugation for 1 min at 10 000 *g*. The resultant *E. coli* pellets were placed in ice-cold PBS supplemented with a mixture of proteinase inhibitors (Complete Mini, Roche Molecular Biochemicals) and 1 mM DTT, homogenized using a glass-Teflon Potter homogenizer, and then centrifuged for 1 h at 4°C at 46 500 *g*. The recombinant GST-fusion proteins in the supernatants were purified using glutathione beads (Glutathione Sepharose 4B, Pharmacia Biotech) in 5 × 50 mm columns (Muromac, Muromachi Kagaku Kogyo Co), according to the manufacturer's instructions. The GST-fusion proteins in the elution buffer were concentrated, and the solvent was substituted using a centrifugal filter (Microcon, Millipore), yielding a final protein concentration of 1 μg ml^{-1} in PBS. To confirm their purity and integrity, protein samples were suspended in Laemmli SDS-PAGE sample buffer, boiled for 10 min, resolved by 12% SDS-PAGE and stained with Coomassie Brilliant Blue (Fig. 7*A*).

The binding of recombinant GST-fusion proteins to PIP_ns was assayed using PIP_ns-coated nitrocellulose membranes (PIP strips, Echelon) according to the manufacturer's instructions. The membranes were first blocked for 30 min at room temperature in TBS-T + 3%BSA blocking solution (20 mM Tris-HCl (pH 8.0), 150 mM NaCl, 0.05% Tween 20 and 3% fatty acid free (BSA), and then incubated with 0.1 μg ml^{-1} samples of the respective proteins in TBS-T + 3%BSA overnight at 4°C. After washing three times with TBS-T + 3%BSA, the membranes were incubated for 2 h at room temperature with goat anti-GST monoclonal antibody diluted in TBS-T + 3%BSA. The membranes were then washed again and incubated for 1 h at room temperature with an anti-goat IgG-HRP secondary antibody diluted in TBS-T + 3% BSA, and then treated with ECL Plus reagent (Amersham Biosciences) to detect the bound GST-fusion proteins. The intensities of the binding spots were quantified using ImageJ image processing software (National Institutes of Health).

Fluorescence assays

COS-7 cells were cultured in Dulbecco's modified Eagle's medium (Nissui Co.) supplemented with 10% fetal bovine serum, 100 us ml^{-1} penicillin, 100 μg ml^{-1} streptomycin,

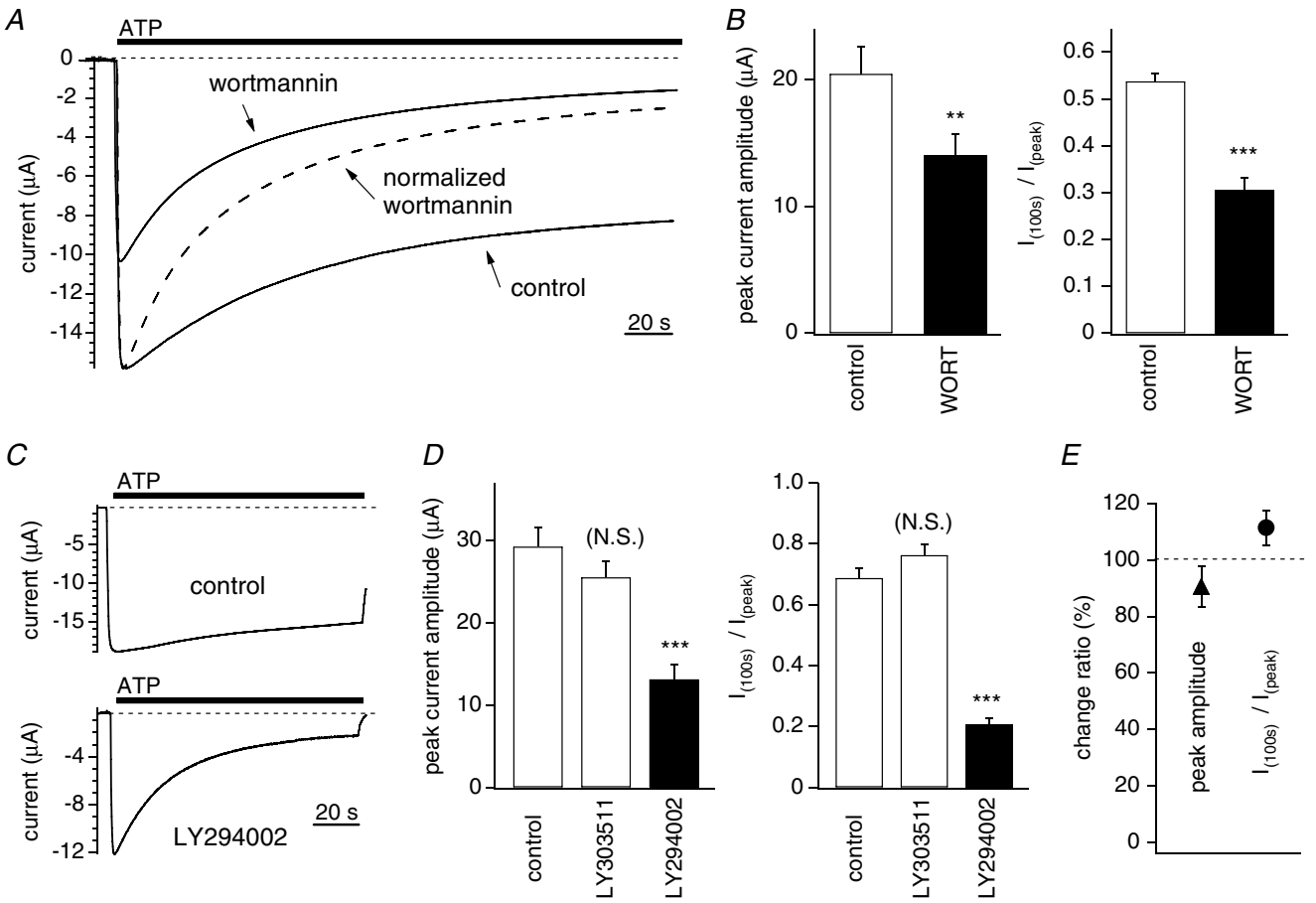

Figure 2. Effect of PI3K inhibitors and G_q-coupled receptor stimulation on desensitization of $P2X_2$ receptor channel

A and *C*, currents carried by WT $P2X_2$ channels expressed in *Xenopus* oocytes were recorded using two-electrode voltage clamp in Na^+-based external solution. The holding potential was −60 mV, and 100 μM ATP was applied. *B*, *D* and *E*, statistical comparison of the peak current amplitudes and the extent of desensitization. The ratios of the current amplitudes measured 100 s after the application of ATP and the peak amplitudes (I_{100s}/I_{peak}) were calculated as an index of desensitization. *A*, representative currents recorded from oocytes with or without preincubation for 2 h with 30 μM wortmannin. Also shown is the normalized current trace obtained with wortmannin. *B*, comparison of the data in *A*. Bars depict means ± S.E.M. ($n = 10$); means were compared statistically using Student's *t* test (***$P < 0.001$, **$P < 0.01$). *C*, representative currents recorded with and without preincubation for 12 h with 30 μM LY294002. *D*, comparison of the data in *C*. Bars depict means ± S.E.M. ($n = 7$–8); means were compared statistically using Tukey's test (***$P < 0.001$ (N.S.): $P > 0.005$). *E*, Peak amplitudes (▲) and I_{100s}/I_{peak} ratios (○) before and after stimulation with 1 μM substance P for 10 min in cells coexpressing $P2X_2$ channels and substance P receptors. Bars depict means ± S.E.M. ($n = 11$).

4 mM glutamine, and 20 mM $NaHCO_3$. The cells were seeded onto poly L-lysine-coated glass coverslips, where they were transiently transfected with EGFP-tagged WT or mutant plasmids using Lipofectamine 2000 (Invitrogen) according to the manufacturer's instructions. After incubation for 24 h, the cells were fixed with 4% paraformaldehyde in PBS for 15 min at room temperature, or with ice-cold 70% ethanol for 3 h. The coverslips were then rinsed three times with PBS, incubated for 5 min with PBS containing 0.5 μg ml^{-1} DAPI, and washed again with PBS. Finally, the coverslips were mounted on slide glass using PermaFluor mounting medium (Shandon).

Fluorescent images were acquired with an AxioCam cooled CCD camera (Zeiss) using a fixed exposure time of 2 s in all experiments. Pseudocolor was added to the digitized images using Photoshop software (Adobe). The fluorescence was quantified using ImageJ software (National Institutes of Health), and pairs of means were statistically compared using Tukey's test.

Results

Effect of phospholipid-disrupting drugs on desensitization of $P2X_2$ channels

Xenopus oocytes were injected with cRNA encoding the rat $P2X_2$ channel, and then incubated for 2–3 days to allow overexpression of the protein. Thereafter they were placed in a perfusion chamber in Na^+-based external solution, and membrane potentials were held at −60 mV using two-electrode voltage clamp. We recorded macroscopic currents from the oocytes before, during and after appling a saturating concentration (100 μM) of ATP to the bath, and analysed the effects of several types of phospholipid-disrupting agents on desensitization (Fig. 2). Zhou *et al.* (1998) reported that the rate of desensitization of $P2X_2$ receptors expressed in either *Xenopus* oocytes or HEK 293 cells varied widely from cell to cell (Zhou *et al.* 1998). To minimize such variation, we recorded from oocytes that were from the same batch and showed similar levels of channel expression. As an index of the intensity of the channel desensitization, we

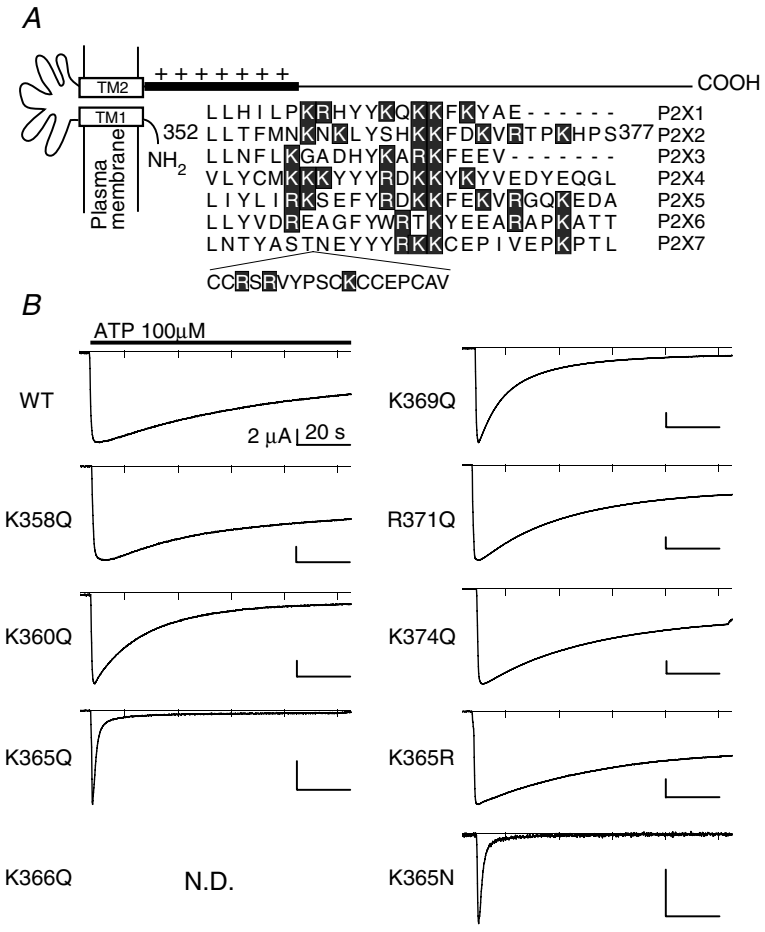

Figure 3. The effect of substituting the positively charged amino acid residues in the proximal region of the cytoplasmic C-terminal domain of $P2X_2$ on desensitization
A, alignment of the amino acid sequences of the proximal C-terminal regions of P2X family proteins. The original reports used for the alignment are as follows: $P2X_1$ (Valera *et al.* 1994), $P2X_2$ (Brake *et al.* 1994), $P2X_3$ (Lewis *et al.* 1995), $P2X_4$ (Seguela *et al.* 1996), $P2X_5$ (Collo *et al.* 1996), $P2X_6$ (Collo *et al.* 1996), $P2X_7$ (Surprenant *et al.* 1996). Positively charged residues (lysine and arginine) are highlighted. *B*, representative macroscopic currents of WT and mutant $P2X_2$ channels recorded as in Fig. 2. N.D. denotes a channel that did not show detectable currents, and so could not be analyzed.

calculated the ratios of the current amplitudes recorded 100 s after application of ATP to the peak amplitudes (I_{100s}/I_{peak}) (Fig. 2*B* and *D*). Macroscopic $P2X_2$ currents showed slow desensitization, with more than 50% of the amplitude remaining 100 s after ATP application (Fig. 2*A* and *B*). This slow desensitization of the $P2X_2$ current was not significantly dependent on the holding potential, the charge carrier (data not shown) or the level of $P2X_2$ expression (Supplemental Fig. 1). Preincubation for 2 h in 30 μM wortmannin, which is known to inhibit PI3K activity, as well as PI4K at high doses, reduced current amplitude and accelerated the desensitization (Fig. 2*A* and *B*), as did preincubation for 12 h with the selective PI3K inhibitor LY294002 (30 μM), but not its negative control reagent, LY303511 (Fig. 2*C* and *D*). The ability of these two PI3K inhibitors to accelerate desensitization was apparent even with shorter incubations. Preincubation for 30 min with wortmannin (30 μM, $n = 6$) or 45 min with LY294002 (30 μM, $n = 10$) reduced I_{100s}/I_{peak} by 23.5% or 20.3%, respectively, as compared to control. Moreover, we suggest that the enhanced desensitization elicited by these drugs overlapped the activation (increasing) phase of the inward current, leading to a reduction in the peak amplitude. Another possibility is that PI3K inhibitors might stimulate internalization of membrane proteins.

To determine the extent to which activation of PLC and the resultant reduction in plasma membrane $PI(4,5)P_2$ levels contributes to desensitization of $P2X_2$ channels, we coexpressed $P2X_2$ and G_q-coupled substance-P receptors in oocytes, and compared the macroscopic $P2X_2$ currents before and after a 10 min incubation in 1 μM substance-P. We found that neither current amplitude nor channel desensitization was altered by this manipulation (Fig. 2*E*). Similarly, following coexpression of G_q-coupled M1 receptors and $P2X_2$, incubation in 100 μM ACh for 10 min had no significant effect on current amplitude or channel desensitization (data not shown). That the coexpressed substance-P or M1 receptors were, in fact, functionally active was confirmed by monitoring the increases in the amplitude of currents through endogenous Ca^{2+}-activated Cl^- channels (supplemental Fig. 2). These results suggest that the desensitization of $P2X_2$ channels is regulated by PI kinase, not PLC. Consequently, a reduction in PI(3)P or $PI(3,5)P_2$ levels, which are regulated by PI3K (Fig. 1), would be expected to have a greater effect on channel desensitization than a reduction in $PI(4,5)P_2$, though the

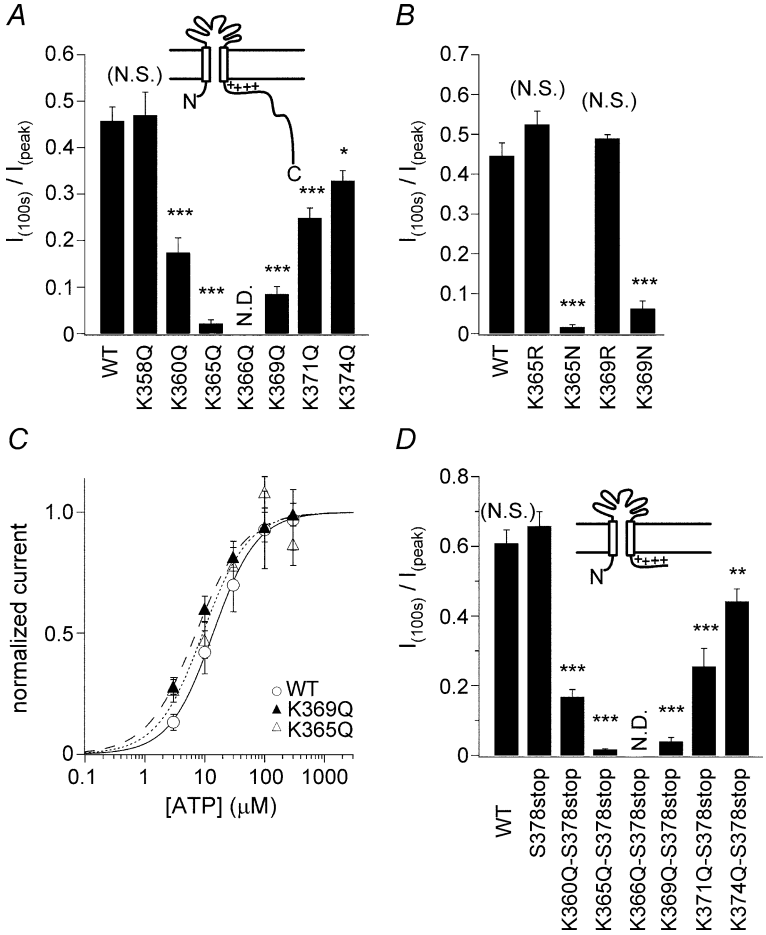

Figure 4. Analysis of the effects of the indicated mutations on the extent of $P2X_2$ channel desensitization

A, *B* and *D*, comparison of the extent in desensitization of WT $P2X_2$ and mutant channels. Currents were recorded as in Fig. 2. Bars depict means ± S.E.M. ($n = 5$–7 in *A*, $n = 7$ in *B* and $n = 5$–10 in *D*); control means (control= WT in *A*, control = WT in *B* and control = S378stop in *D*) and those of each mutant were compared statistically using Tukey's test (***$P < 0.001$, **$P < 0.01$, *$P < 0.05$ and (N.S) means $P > 0.05$). *C*, concentration–response relationships of WT $P2X_2$ and the indicated mutants.

latter is known to be involved in regulating the activity of a variety of ion channels.

Structural background for the regulation $P2X_2$ channels by PIP_ns

All PIP_ns are anionic lipids and are expected to interact with positive charges on the $P2X_2$ protein. The proximal region of the cytoplasmic C-terminal domain contains a cluster of positively charged amino acids that are highly conserved among P2X family members and would seem to be likely sites of interaction with PIP_ns (Fig. 3*A*). We therefore constructed several $P2X_2$ mutants in which those positively charged amino acids were substituted, one at a time, and then analysed the mutants' capacity to affect desensitization. We did not quantitatively compare the current amplitudes obtained with the different constructs, because the expression levels were dependent on the quality of each *in vitro*-translated cRNA, which is difficult to control precisely. Macroscopic currents were recorded from oocytes (Fig. 3*B*) and compared (Fig. 4*A*) as in Fig. 2. With the exception of K358Q, all neutralizing point mutations (K360Q, K365Q, K369Q, R371Q and K374Q) accelerated desensitization, and the K366Q mutant did not carry any detectable current at all (Figs 3*B* and 4*A*). This loss of function might have been due to a trafficking disorder, as the mutation was in a region that includes a trafficking motif (Y_{362}xxxK_{366}) (Chaumont *et al.* 2004). K365R and K369R each desensitized as slowly as the WT channel, while K365N and K369N showed faster desensitization (Fig. 4*B*). We also observed that the ATP concentration–response relationships were not significantly altered in the rapidly desensitizing mutants (the K_d values were 13.8 μM ($n = 5$) for the WT channel, 9.3 μM ($n = 5$) for K365Q, and 7.2 μM ($n = 5$) for K369Q), which confirmed that the concentration of ATP used (100 μM) was saturating for all of the mutants as well as for the WT channel. As the distal region of the C-terminal domain has been reported to cooperate with the proximal region to determine the extent of desensitization (Smith *et al.* 1999), we also made deletion mutants and analysed their effect on desensitization. Addition of a K360Q, K365Q, K369Q, R371Q or K374Q mutation to a background of S378stop accelerated desensitization to an extent similar to that seen when the mutations were added to the WT channel (Fig. 4*D*). These results imply that just the proximal region of the C-terminus cytoplasmic domain including the positively charged residues electrostatically prevents the channel desensitization.

From the sequence alignment shown in Fig. 3*A*, we noticed that two important positively charged amino acid residues, K369 and R371, are not conserved in $P2X_4$ (Y374 and E376), which is known to show rapid desensitization. To test the possibility that the rapid desensitization of $P2X_4$ is due to the absence of these two positively charged amino acids, we made Y374K, E376R and Y374K/E376R mutants. The WT $P2X_4$ channel showed a biphasic current comprised of an initial 'desensitizing component' that was followed by a 'gradually increasing component' (Fig. 5*A*), and no alterations in desensitization were observed in the mutants (Fig. 5*B* and *C*). In this study, we decided to focus on just the $P2X_2$ channel rather than to expand to other members, and proceeded to the study further in the following. The data summarized in Figs 2–4 suggest that anionic PIP_ns electrostatically interact with cationic residues in the proximal C-terminal region of the cytoplasmic C-terminal domain of the $P2X_2$ channel, thereby inhibiting channel desensitization.

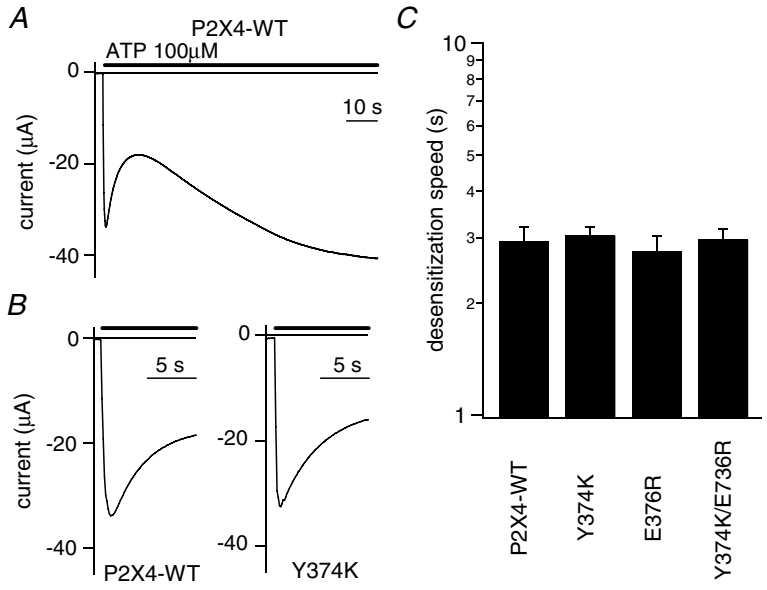

Figure 5. Effects on desensitization of introducing positively charged amino acid residues into the C-terminal domain of $P2X_4$
A, representative current through the WT $P2X_4$ channel. An initial fast desensitization phase and a later slow resensitization phase were observed. *B*, expanded recordings of the desensitization phase of WT $P2X_4$ and the Y374K mutant. *C*, comparison of the speed of desensitization of WT and mutant $P2X_2$ channels. I_{100s}/I_{peak} was not usable as an index here, so the desensitization phase was fitted with a single exponential function, and the time constants were determined. Bars depict means ± S.E.M. ($n = 7$).

Because the changes elicited by K365Q and K369Q neutralizing point mutations were the most remarkable, we used these mutants as representative in the following experiments.

Correlation of changes in ion selectivity with channel desensitization

A unique property of P2X channels is that their permeability to large cations time dependently increases following ATP binding, which suggests that a conformational change leading to a sort of pore dilation takes place. Because desensitization of the channel also reflects conformational changes after ATP application, we next correlated changes in NMDG permeability with desensitisation, and examined the effects of K365Q and K369Q mutation and PI3K inhibition.

We previously reported that increases in the permeability to large cations are more apparent in oocytes expressing high levels of $P2X_2$ (Fujiwara & Kubo, 2004). For this analysis therefore we selected oocytes showing high levels of expression, which enabled clear detection of the changes of ion selectivity. The values of the peak inward current amplitudes (mean ± S.E.M.) in Na^+-based external solution at −30 mV were 17.0 ± 1.6 μA (WT control, $n = 5$), 19.1 ± 2.2 μA (K369Q, $n = 7$), 19.7 ± 3.2 μA (K365Q, $n = 7$) and 11.5 ± 1.4 μA (WT preincubated with wortmannin ($n = 4$). We then applied a saturating concentration of ATP (100 μM) to oocytes in NMDG-based external solution, and obtained current–voltage (I–V) relationships by applying ramp pulses every 0.5 s for 90 s after ATP application (Fig. 6*A*). Also shown are the currents recorded at −90 mV (insets).

The desensitization that occurred in NMDG-based external solution was similar to that seen in Na^+-based solution in Figs 2–4 (Fig. 6*A*, inset). After application of ATP to WT oocytes, the reversal potential initially remained at a hyperpolarized potential (∼−78 mV), but progressively shifted toward more depolarized potentials (black traces in Fig. 6*A*). After this phase, a slow, but exact, recovery of the reversal potential toward hyperpolarization (blue traces in Fig. 6*A*) was observed (Fig. 6*A* and *B*). This suggests that the channel was permeable primarily to small cations immediately after application of ATP, and that the permeability to a large cation, NMDG, increased gradually but then slowly declined, while the permeability to small cations remained. A series of changes in the reversal potential in NMDG-based external solution were observed both in WT with or without wortmannin preincubation, and in the mutants (Fig. 6*A*). Although the recovery of reversal potential to hyperpolarization as well as the desensitization was very slow in WT, a series of changes observed were qualitatively similar, suggesting that the relationship of the two processes of pore dilation and desensitization was not altered by the desensitizing manipulations (Figs 2–4). Preincubation in wortmannin, which accelerated desensitization (Fig. 2), also accelerated the recovery from the shift in the reversal potential (Fig. 6*A* and *B*). Moreover, the rapidly desensitizing K369Q and K365Q mutants (Figs 3 and 4) also showed accelerated recovery from the shift of the reversal potential (Fig. 6*A* and *B*). The respective time constants for the recovery phase of the reversal potential (Fig. 6*B*) and for the reduction in current amplitude at −90 mV (i.e. desensitization) in NMDG-based external solution (Fig. 6*A*, inset) were obtained by fitting the data with a single exponential function, and are plotted in Fig. 6*C*. With the WT channel, the recovery of the reversal potential was too slow to be analysed precisely. Accumulative data plotted in Fig. 6*C* showed that the speed of recovery was strongly correlated with the speed of desensitization in NMDG-based external solution (Fig. 6*C*). We also carried out similar experiments using oocytes expressing low or medium levels of $P2X_2$, and observed similar tendencies (data not shown).

There is thus a clear correlation between the recovery of the shift in reversal potential after application of ATP and channel desensitization. In addition, the fact that the open channels remaining during the desensitization phase showed more hyperpolarized reversal potentials suggests that open channels with large pores tend to desensitize faster than channels with small pores.

Binding of the $P2X_2$ proximal C-terminal region to phospholipids

We next used PIP_n-coated nitrocellulose membranes to analyse the binding to anionic lipids of GST-tagged recombinant $P2X_2$ channel fragments comprising the proximal cytoplasmic region (L353 to S377). For this experiment, we prepared six samples: GST protein alone (negative control), the WT protein and four mutants, all tagged with GST. Approximately equivalent amounts of all six proteins were incubated with the membrane (Fig. 7*A*), and tight binding between a GST-fusion protein and the phospholipids appeared as a binding spot (Fig. 7*C*). Also shown are representative current traces obtained with the WT and mutant $P2X_2$ channels. The WT protein selectively bound to PIPs and PIP_2s, especially to PIPs, $PI(3,4)P_2$ and $PI(3,5)P_2$, but not to other negatively charged lipids such as phosphatidyl serine (PS) and PI. The K365Q and K369Q mutations, which accelerated desensitization, showed significantly reduced binding to PIP_ns, whereas the K365R mutation caused a slight reduction in the intensity of binding spots, but the pattern of the spots was similar to that seen with the WT protein. The intensities of the binding spots were quantified using image processing software (black-intensity $pixel^{-1}$, means ± S.E.M., $n = 2$–3) and were as follows, PI(4)P:

161 ± 19 (WT), 104 ± 4 (K365R), 13 ± 5 (K365Q) and PI(3,5)P_2: 93 ± 4 (WT), 48 ± 5 (K365R), 13 ± 2 (K365Q). No binding spots were observed with the non-functional K366Q mutant. We also carried out strip assays using a GST-tagged 'whole' cytoplasmic domain from the WT channel (L353 to L472), and observed binding spots similar to those obtained with the recombinant WT protein. There was, however, a high level of background noise, which may have been caused by contaminating proteins due to insufficient purification. All assays were carried out more than twice, and similar results were reproducibly observed. These findings further substantiate the idea that PIPs and PIP_2s directly bind to the proximal region of the C-terminal cytoplasmic domain of the $P2X_2$ channel, thereby modulating the rates of channel desensitization and recovery from pore dilation.

Association of the $P2X_2$ C-terminal domain with the plasma membrane

Using a cell permeabilization technique involving fixation with ethanol, Chemin *et al.* (2005) were able to determine

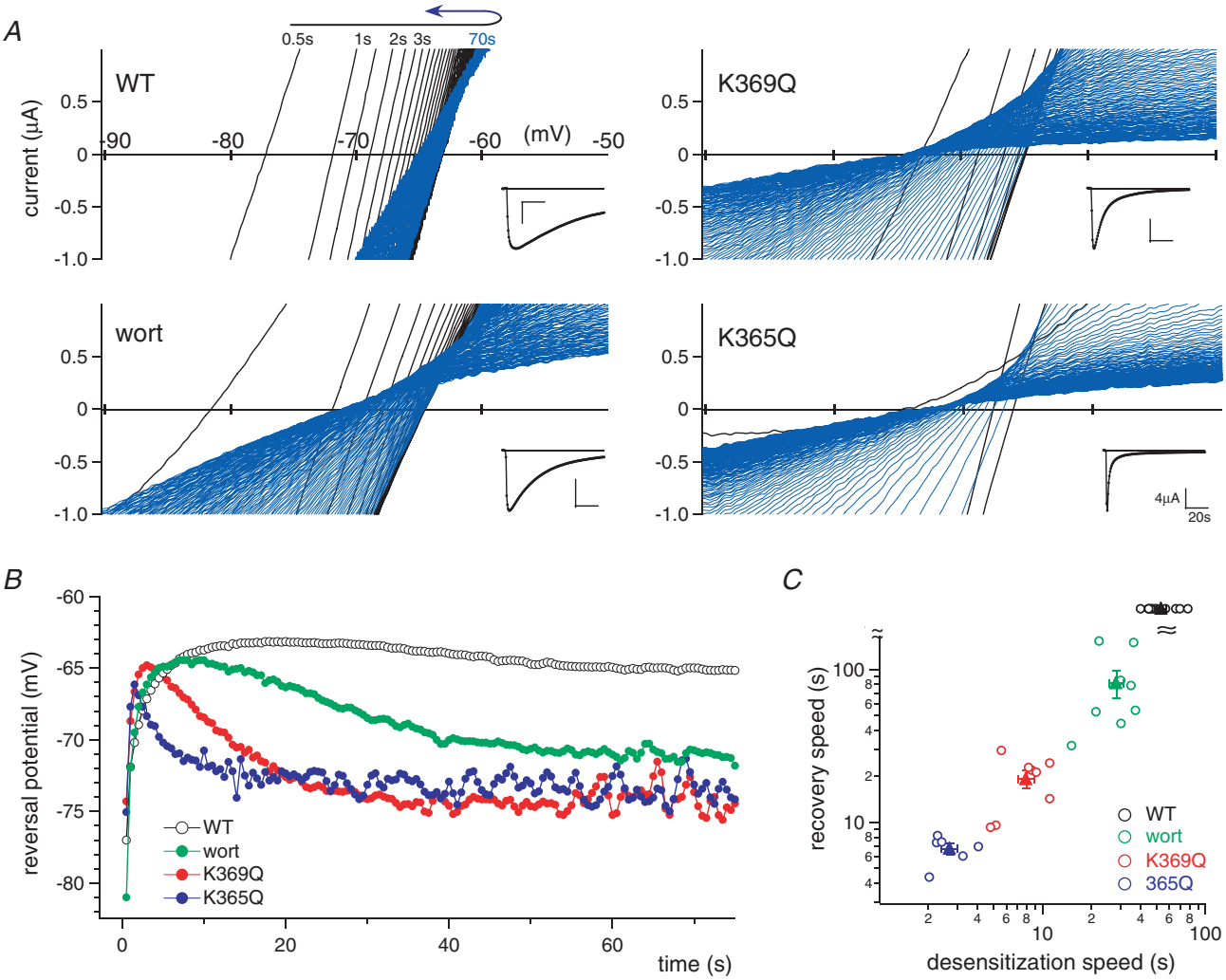

Figure 6. The relationship between channel desensitization and the time-dependent changes in the permeability to NMDG

A, representative time-dependent changes in the current–voltage relationships in NMDG-based solution after ATP application. Recordings were obtained by applying ramp pulses every 0.5 s to oocytes expressing WT or mutant $P2X_2$ receptors. The inset shows current traces measured at −90 mV. In each recording, shifts in the direction of depolarization are shown in black, while shifts in the direction of hyperpolarization (recovery) are shown in blue. *B*, time-dependent shifts in the reversal potentials derived from the data in *A*. The symbols used are as indicated in the figure, wort = wortmannin. *C*, relationship between the speed of recovery of the shift in the reversal potential and the speed of the reduction in current amplitude (desensitization) in NMDG-based external solution. The time constants of the recovery are plotted against those of the desensitization for each of the oocytes recorded (*C*, open circles). Filled triangles and bars depict means ± S.E.M. of each group ($n = 11$ (WT), $n = 8$ (wort), $n = 8$ (K369Q) and $n = 6$ (K365Q)).

that the cytoplasmic domain of the TREK-1 channel interacts with the plasma membrane. We applied the same technique to test whether the C-terminus of $P2X_2$ is able interact with the plasma membrane via membrane-bound PIP_ns. Five constructs were made encoding fusion proteins comprising the fluorescent protein EGFP, and various regions of the $P2X_2$C-terminal domain. These included EGFP plus the entire cytoplasmic C-terminal domain (L353–L472), the proximal region (L353–S378stop), the distal region (S378–L472), and the proximal region carrying a K365Q or K365R mutation (indicated in Fig. 8*A*). EGFP alone served as a negative control.

The constructs were transiently expressed in COS-7 cells, which were then fixed in either paraformaldehyde(PFA) or ice-cold ethanol. With the latter, cytoplasmic proteins not bound to the plasma membrane or an organelle membrane leaked from the cell (Fig. 8*A*). The EGFP signals were recorded using the same exposure time for all constructs (2 s), and the accumulated data are summarized in Fig. 8*B*. As expected, fixation with permeabilization in ethanol led to a loss of fluorescence from cells transfected with the control EGFP (Fig. 8*A*, EGFP alone). By contrast, an intense EGFP signal was retained by cells transfected with the full-length C-terminus or the proximal C-terminal region (Fig. 8*A* and *B*, whole and proximal). With the distal C-terminal region, but contrast, the fluorescence was diminished to the level of the negative control (Fig. 8*A* and *B*, distal). K365Q mutation in the proximal region also significantly reduced signal intensity (Fig. 8*A* and *B*, proximal K365Q), whereas the signal in the K365R mutant clearly persisted (Fig. 8*A* and *B*, proximal K365R). Thus the proximal region of the $P2X_2$ cytoplasmic C-terminal domain, which was shown to bind to the immobilized phospholipids on a nitrocellulose-sheet, also is able to associate with the cell membrane, probably by interacting with PIP_ns.

Discussion

In this study we used electrophysiological, biochemical and cell biological approaches to analyse the regulation of $P2X_2$ channel function by PIP_ns bound to the proximal cytoplasmic region of the channel. We also revealed for the first time that desensitization of the channel and pore dilation are correlated, and that both are regulated by the binding of PIP_ns.

Dynamic regulation of channel activity by phosphoinositides

Regulation of channel activity by PIP_ns has been reported for a variety of ion channels. Particularly well studied because their physiological significance are the Kir and KCNQ channels, in which $PI(4,5)P_2$ is a key regulator of the number of active channels, and K^+ conductance is reduced upon stimulation of G_q-coupled receptors, which

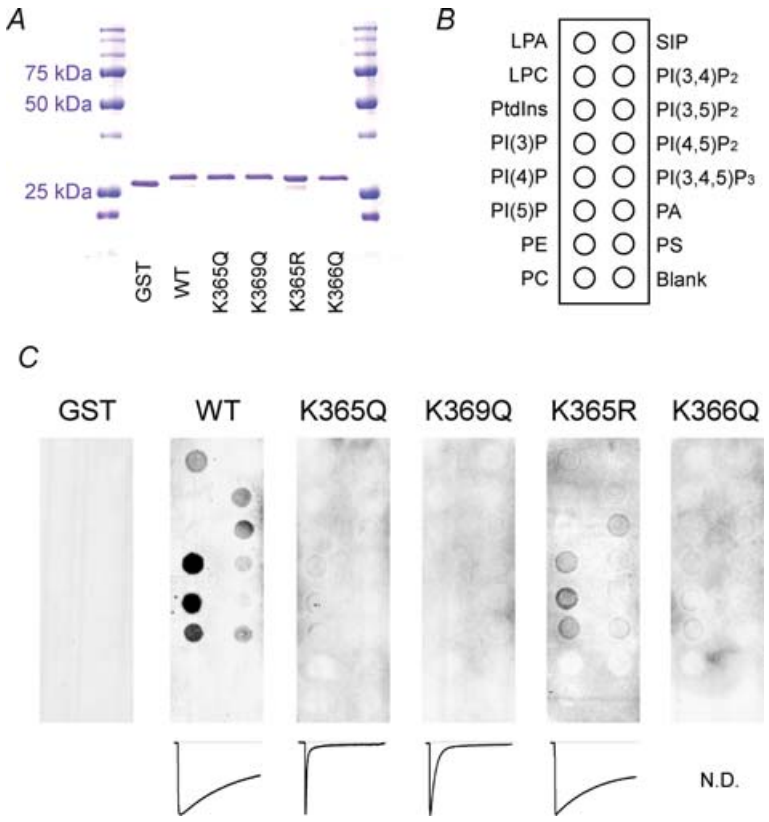

Figure 7. Binding of the proximal region of the $P2X_2$ cytoplasmic C-terminal domain to phospholipids
A, recombinant GST-tagged WT and mutant proximal C-terminal regions of $P2X_2$ were resolved by SDS-PAGE and stained with Coomassie Brilliant Blue. *B*, positions of the indicated phospholipids blotted on a nitrocellulose membrane. Abbreviations used are as follows: Lyso phosphatidic acid (LPA); lysophosphocholine (LPC); sphingosine-1-phosphate (SIP); phosphatidic acid (PA); phosphatidyl choline (PC); phosphatidyl serine (PS); phosphatidyl ethanolamine (PE). *C*, binding patterns of the WT and K365Q, K369Q, K365R K366Q mutant proteins and a negative control protein (GST) to phospholipids blotted on the membrane.

causes breakdown of $PI(4,5)P_2$ (Huang *et al.* 1998; Suh & Hille, 2002; Zhang *et al.* 2003). However, the regulation of $P2X_2$ by PIP_ns that we observed in the present study clearly differs in two respects from the way in which Kir or KCNQ channels are regulated.

First, PI(3)P and $PI(3,5)P_2$, rather than $PI(4,5)P_2$, appear to be the main regulators of $P2X_2$ function, taking the PIP_ns metabolism (Fig. 1) into consideration. We found that desensitization of $P2X_2$ was not induced by the stimulation of G_q-coupled receptors, but by pharmacological inhibition of PI3K activity. We also observed remarkable binding of PI and $PI(3,5)P_2$, but not $PI(4,5)P_2$, to the channel, although we could not identify in detail the contribution made by each PIP_n. There are earlier reports showing the dependence of channel activity on PIP_ns other than $PI(4,5)P_2$. For instance, the small-conductance Ca^{2+}-activated K^+ channel, whose activity also is affected by PI3K, is regulated by PI(3)P and $PI(3,5)P_2$ (Srivastava *et al.* 2005), while cyclic nucleotide-gated (Zhainazarov *et al.* 2004) and epithelial Na^+ channels (Pochynyuk *et al.* 2005) are regulated by $PI(3,4,5)P_3$.

The second unique feature of the regulation of $P2X_2$ function is that PIP_ns did not merely alter the number of active channels, but dynamically affected the gating of the channel after opening by ATP. We observed that channel desensitization was accelerated by a reduction in PIP_ns, which suggests that PIP_n binding prevents the open channel from entering the desensitized state. If PIP_n binding simply determined the number of live or active channels, reducing PIP_ns would only reduce current amplitude. That PIP_ns also are related to the

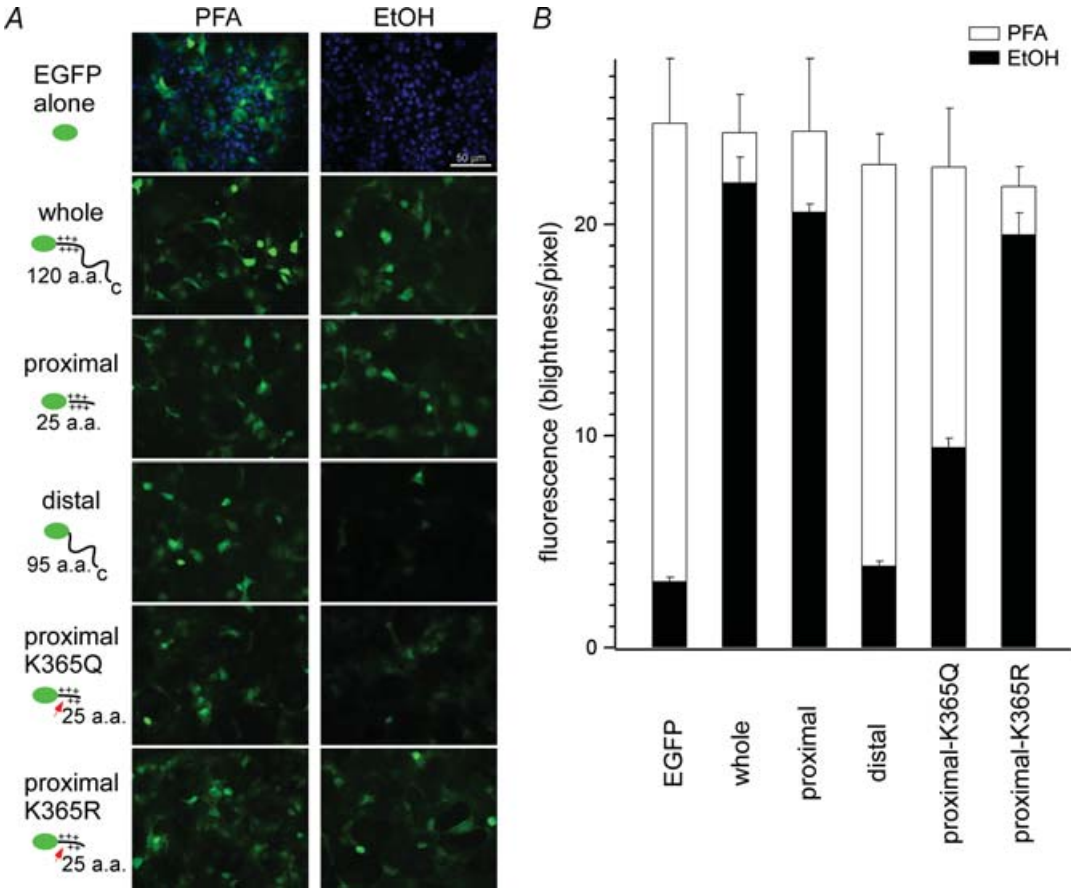

Figure 8. Interaction of the $P2X_2$ cytoplasmic C-terminal domain with the plasma membrane
A, expression of EGFP and EGFP-$P2X_2$ fusion proteins in transiently transfected COS-7 cells. The abbreviations used are as follows: EGFP alone, EGFP protein used as a negative control; whole, EGFP with the entire cytoplasmic C-terminus (L353–L472); proximal, EGFP with the proximal C-terminal region (L353–S378stop); distal, EGFP with the distal C-terminal region (S378–L472); proximal K365Q or K365R, EGFP with the proximal C-terminus carrying the K365Q or K365R mutation, respectively. Cells were fixed in either paraformaldehyde or ethanol. Images were acquired with a 20× objective lens and an optical filter set for EGFP. In the images of EGFP alone, DAPI staining also is shown to confirm that there are sufficient numbers of cells in the visual field. The cell density is similar in the other images, but DAPI staining was omitted for clarity. *B*, quantitative comparison of the intensity of the fluorescence signals obtained with the indicated five constructs.

time-dependent changes in the permeability to NMDG suggests PIP_ns are able to modulate the state transitions after the channel opening.

Structural background of desensitization and pore dilation

Several earlier studies have focused on the involvement of the P2X cytoplasmic C-terminal domain in determining the rate and extent of desensitization. That this region is important for the desensitization of $P2X_2$ channels was first suggested by the observed differences in the phenotypes of the WT channel and a V370 splice variant (Koshimizu *et al.* 1999; Smith *et al.* 1999). Based on analysis of various P2X mutants and chimeras, it was concluded that the positively charged region of the domain was critical for desensitization (Koshimizu *et al.* 1999; Smith *et al.* 1999). We therefore evaluated direct binding of lipids to the channel, and observed that PIP_ns, but not other negatively charged lipids (e.g. PS or PI), bind to the proximal region of the cytoplasmic C-terminal domain when key positive charges are intact. This suggests that the binding of membrane PIP_ns to the C-terminal domain plays a key role in preventing channel desensitization. Two earlier findings that also suggest the importance of PIP_ns and PI3K in the regulation of desensitization are that desensitization is accelerated in outside-out excised patches (Zhou & Hume, 1998), and that the rate of desensitization of the $P2X_2$ channel varies from cell to cell (Zhou *et al.* 1998).

One might thus expect that the rapid desensitization of $P2X_{1,3,4}$ is the result of reduced binding of PIP_ns to the proximal region of the C-terminal domain; indeed K369 and R371, two positively charged amino acid residues found in $P2X_2$, are not conserved in these channels. We therefore tested the effect on desensitization of substituting positively charged amino acid(s) at the corresponding site of $P2X_4$, yielding the Y374K and/or E736R mutants (Fig. 5). However, the speed of desensitization of the mutants did not differ from that of the WT channel. It may be that not only the charge, but also total conformation of this region is critical for deceleration of desensitization. If so, perhaps this question could be addressed using chimeras containing all or various parts of the proximal C-terminal region. Alternatively, it may be that the mechanisms underlying desensitization are complex and differ in $P2X_2$ and $P2X_4$.

We also analysed a unique property of the P2X channel pore: the time-dependent change in its permeability to NMDG. The time-dependent increase in the permeability to NMDG implies that pore size gradually increases after ATP binds to the channel. This phenomenon, called 'pore dilation' (Virginio *et al.* 1999), is reportedly caused by rearrangement of the transmembrane conformation (Khakh & Egan, 2005). We observed that the increase in NMDG permeability was rapidly reversed when channel desensitization was accelerated by mutation or inhibition of PI3K (Fig. 6). Apparently, recovery from pore dilation is closely linked to channel desensitization and also is regulated by the binding of PIP_ns to the cytoplasmic C-terminal region of the channel. The kinetics of pore dilation, which can be derived from the data of the initial depolarizing-shift in reversal potential (Fig. 6*B*),

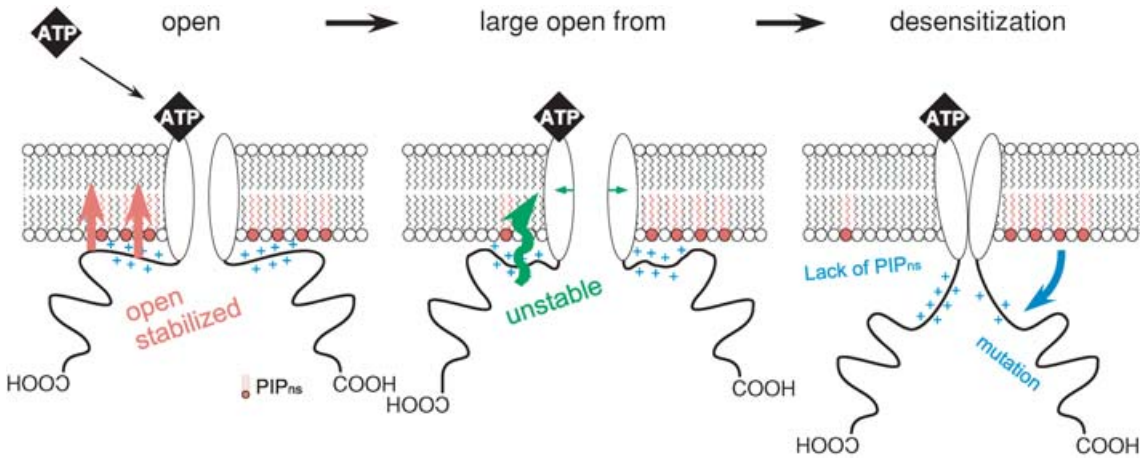

Figure 9. Schematic diagram explaining the membrane PIP_n-dependent conformational changes in the $P2X_2$ channel

For convenience, only the cytoplasmic C-terminal domain and the transmembrane pore region of the channel are shown; omitted are the extracellular domain and the cytoplasmic N-terminal region. Open: an initial open state with a low permeability to NMDG. Large open form: a state showing a high permeability to NMDG. The equilibrium is inclined toward the desensitized state when interaction with the plasma membrane is not maintained. Conformational changes in the proximal cytoplasmic region are thought to occur during transitions from the open to the large open state, and from large open to the desensitized state.

also were accelerated by these manipulations. The means and S.E.M. values of the time constants were as follows, WT: 3.95 ± 0.40 s ($n = 12$), wortmannin: 2.71 ± 0.22 s ($n = 10$), K369Q: 2.10 ± 0.41 s ($n = 9$, $P < 0.01$ *versus* WT), K365Q: 1.08 ± 0.22 s ($n = 6$, $P < 0.001$ *versus* WT). Although these kinetics could be indirectly influenced by the declining phase (i.e. when the declining phase is fast, the slowly increasing phase will be masked, which would affect the fitting used for time constant evaluation) and quantitative uncertainties remain, it is clear that the kinetics of pore dilation also are accelerated by the same mutations and inhibition of PI3K that accelerated desensitization. This suggests that pore dilation too is influenced by the binding of PIP_ns to the proximal C-terminal region. Consistent with that idea are the findings of an earlier mutagenesis study that showed the cytoplasmic tail of $P2X_2$ to play an important role in pore dilation (Khakh & Lester, 1999; Eickhorst *et al.* 2002) and a fluorescence resonance energy transfer (FRET)-based analysis that showed this region to move during the pore dilation (Fisher *et al.* 2004). In addition, Jiang *et al.* (2005) reported that the cysteine-rich region situated between the transmembrane domain and the conserved proximal C-terminal region (Fig. 2*A*), is critical for the large open conformation of the $P2X_7$ channel. It thus appears to us that the proximal region of the cytoplasmic C-terminal domain plays a key role in the regulation of both the channel desensitization and pore dilation by PIP_ns.

Proposed model of $P2X_2$ channel gating

One model that can explain the link between desensitization and pore dilation is illustrated schematically in Fig. 9. The drawing summarizes the dynamic changes in $P2X_2$ pore properties regulated by PIP_ns. We assume the presence of three conformational states after the channel opening elicited by ATP binding: open with a small pore (left), open with a dilated pore (middle) and desensitized (right). As discussed in the previous section, the reduction in NMDG-permeability – i.e. recovery of the reversal potential – correlated with channel desensitization (Fig. 6). If the desensitization occurred mainly from the small pore, the reversal potential would not clearly shift towards hyperpolarization, and the shift of the reversal potential would not be influenced as shown in Fig. 6*B* and *C* by the desensitizing manipulations such as mutations and preincubation in wortomannin. The results imply that the channels desensitize dominantly from the large pore state. We therefore hypothesize that the large open conformation is adjacent to the desensitized state.

In the WT channel, the proximal cytoplasmic C-terminal domain, with its positive charges, tightly binds anionic PIP_ns in the plasma membrane, stabilizing the large open pore conformation and thus decelerating desensitization (Fig. 6*B*, ○). If the level of membrane PIP_ns is reduced or the key positive charges in the proximal cytoplasmic region are removed by mutation, the anchor with the plasma membrane becomes unstable, and conformational changes occur that lead to the desensitized state (Fig. 9). In addition, the conformations of the proximal cytoplasmic region in the small and large open states also would be expected to differ from one another, as manipulation of PIP_n binding also affected the speed of pore dilation (Fig. 6*B*). Such a conformational change during pore dilation has been detected previously using FRET analysis (Fisher *et al.* 2004) and in other studies. Further structure biological analyses will be necessary to clarify the details of the two conformational changes proposed in this model.

In summary, we propose that the conformational changes of the transmembrane regions in the pore dilation and in the desensitization are caused by the rearrangement of the cytoplasmic region, particularly the proximal domain that is linked with the plasma membrane via PIP_ns. This long-range effect in protein from the cytoplasmic region may modulate the transmembrane channel gating (Werner *et al.* 1996; Khakh & Egan, 2005), as reported for other ion channels (Minor *et al.* 2000; Bichet *et al.* 2004).

References

Baukrowitz T, Schulte U, Oliver D, Herlitze S, Krauter T, Tucker SJ, Ruppersberg JP & Fakler B (1998). PIP2 and PIP as determinants for ATP inhibition of KATP channels. *Science* **282**, 1141–1144.

Bichet D, Lin YF, Ibarra CA, Huang CS, Yi BA, Jan YN & Jan LY (2004). Evolving potassium channels by means of yeast selection reveals structural elements important for selectivity. *Proc Natl Acad Sci U S A* **101**, 4441–4446.

Brake AJ, Wagenbach MJ & Julius D (1994). New structural motif for ligand-gated ion channels defined by an ionotropic ATP receptor. *Nature* **371**, 519–523.

Chaumont S, Jiang LH, Penna A, North RA & Rassendren F (2004). Identification of a trafficking motif involved in the stabilization and polarization of P2X receptors. *J Biol Chem* **279**, 29628–29638.

Chemin J, Patel AJ, Duprat F, Lauritzen I, Lazdunski M & Honore E (2005). A phospholipid sensor controls mechanogating of the K^+ channel TREK-1. *EMBO J* **24**, 44–53.

Collo G, North RA, Kawashima E, Merlo-Pich E, Neidhart S, Surprenant A & Buell G (1996). Cloning OF P2X5 and P2X6 receptors and the distribution and properties of an extended family of ATP-gated ion channels. *J Neurosci* **16**, 2495–2507.

Corvera S (2001). Phosphatidylinositol 3-kinase and the control of endosome dynamics: new players defined by structural motifs. *Traffic* **2**, 859–866.

Czirjak G, Petheo GL, Spat A & Enyedi P (2001). Inhibition of TASK-1 potassium channel by phospholipase C. *Am J Physiol Cell Physiol* **281**, C700–C708.

Ding S & Sachs F (2000). Inactivation of P2X2 purinoceptors by divalent cations. *J Physiol* **522**, 199–214.

Donaldson MR, Jensen JL, Tristani-Firouzi M, Tawil R, Bendahhou S, Suarez WA, Cobo AM, Poza JJ, Behr E, Wagstaff J, Szepetowski P, Pereira S, Mozaffar T, Escolar DM, Fu YH & Ptacek LJ (2003). PIP2 binding residues of Kir2.1 are common targets of mutations causing Andersen syndrome. *Neurology* **60**, 1811–1816.

Eickhorst AN, Berson A, Cockayne D, Lester HA & Khakh BS (2002). Control of P2X (2) channel permeability by the cytosolic domain. *J Gen Physiol* **120**, 119–131.

Fisher JA, Girdler G & Khakh BS (2004). Time-resolved measurement of state-specific P2X2 ion channel cytosolic gating motions. *J Neurosci* **24**, 10475–10487.

Fujiwara Y & Kubo Y (2002). Ser165 in the second transmembrane region of the Kir2.1 channel determines its susceptibility to blockade by intracellular Mg^{2+}. *J Gen Physiol* **120**, 677–693.

Fujiwara Y & Kubo Y (2004). Density-dependent changes of the pore properties of the P2X2 receptor channel. *J Physiol* **558**, 31–43.

Hardie RC, Raghu P, Moore S, Juusola M, Baines RA & Sweeney ST (2001). Calcium influx via TRP channels is required to maintain PIP2 levels in *Drosophila* photoreceptors. *Neuron* **30**, 149–159.

Hilgemann DW, Feng S & Nasuhoglu C (2001). The complex and intriguing lives of PIP2 with ion channels and transporters. *Sci STKE* **2001(111)**, RE19.

Huang CL, Feng S & Hilgemann DW (1998). Direct activation of inward rectifier potassium channels by PIP2 and its stabilization by Gbetagamma. *Nature* **391**, 803–806.

Inoue K, Tsuda M & Koizumi S (2004). ATP- and adenosine-mediated signaling in the central nervous system: chronic pain and microglia: involvement of the ATP receptor P2X4. *J Pharmacol Sci* **94**, 112–114.

Jiang LH, Rassendren F, Mackenzie A, Zhang YH, Surprenant A & North RA (2005). *N*-methyl-D-glucamine and propidium dyes utilize different permeation pathways at rat P2X (7) receptors. *Am J Physiol Cell Physiol* **289**, C1295–C1302.

Khakh BS, Bao XR, Labarca C & Lester HA (1999*a*). Neuronal P2X transmitter-gated cation channels change their ion selectivity in seconds. *Nat Neurosci* **2**, 322–330.

Khakh BS & Egan TM (2005). Contribution of transmembrane regions to ATP-gated P2X2 channel permeability dynamics. *J Biol Chem* **280**, 6118–6129.

Khakh BS & Lester HA (1999). Dynamic selectivity filters in ion channels. *Neuron* **23**, 653–658.

Khakh BS, Proctor WR, Dunwiddie TV, Labarca C & Lester HA (1999*b*). Allosteric control of gating and kinetics at P2X (4) receptor channels. *J Neurosci* **19**, 7289–7299.

Koshimizu T, Koshimizu M & Stojilkovic SS (1999). Contributions of the C-terminal domain to the control of P2X receptor desensitization. *J Biol Chem* **274**, 37651–37657.

Lewis C, Neidhart S, Holy C, North RA, Buell G & Surprenant A (1995). Coexpression of P2X2 and P2X3 receptor subunits can account for ATP-gated currents in sensory neurons. *Nature* **377**, 432–435.

Liou HH, Zhou SS & Huang CL (1999). Regulation of ROMK1 channel by protein kinase A via a phosphatidylinositol 4,5-bisphosphate-dependent mechanism. *Proc Natl Acad Sci U S A* **96**, 5820–5825.

Lopes CM, Zhang H, Rohacs T, Jin T, Yang J & Logothetis DE (2002). Alterations in conserved Kir channel–PIP2 interactions underlie channelopathies. *Neuron* **34**, 933–944.

Minor DL, Lin YF, Mobley BC, Avelar A, Jan YN, Jan LY & Berger JM (2000). The polar T1 interface is linked to conformational changes that open the voltage-gated potassium channel. *Cell* **102**, 657–670.

North RA (2002). Molecular physiology of P2X receptors. *Physiol Rev* **82**, 1013–1067.

Oliver D, Lien CC, Soom M, Baukrowitz T, Jonas P & Fakler B (2004). Functional conversion between A-type and delayed rectifier K^+ channels by membrane lipids. *Science* **304**, 265–270.

Pochynyuk O, Staruschenko A, Tong Q, Medina J & Stockand JD (2005). Identification of a functional phosphatidylinositol 3,4,5-trisphosphate binding site in the epithelial Na^+ channel. *J Biol Chem* **280**, 37565–37571.

Prestwich GD (2004). Phosphoinositide signaling; from affinity probes to pharmaceutical targets. *Chem Biol* **11**, 619–637.

Ralevic V & Burnstock G (1998). Receptors for purines and pyrimidines. *Pharmacol Rev* **50**, 413–492.

Schulte U, Hahn H, Konrad M, Jeck N, Derst C, Wild K, Weidemann S, Ruppersberg JP, Fakler B & Ludwig J (1999). pH gating of ROMK (K(ir)1.1) channels: control by an Arg-Lys-Arg triad disrupted in antenatal Bartter syndrome. *Proc Natl Acad Sci U S A* **96**, 15298–15303.

Seguela P, Haghighi A, Soghomonian JJ & Cooper E (1996). A novel neuronal P2x ATP receptor ion channel with widespread distribution in the brain. *J Neurosci* **16**, 448–455.

Shyng SL & Nichols CG (1998). Membrane phospholipid control of nucleotide sensitivity of KATP channels. *Science* **282**, 1138–1141.

Smith FM, Humphrey PP & Murrell-Lagnado RD (1999). Identification of amino acids within the P2X2 receptor C-terminus that regulate desensitization. *J Physiol* **520**, 91–99.

Srivastava S, Li Z, Lin L, Liu G, Ko K, Coetzee WA & Skolnik EY (2005). The phosphatidylinositol 3-phosphate phosphatase myotubularin- related protein 6 (MTMR6) is a negative regulator of the Ca^{2+}-activated K^+ channel KCa3.1. *Mol Cell Biol* **25**, 3630–3638.

Suh BC & Hille B (2002). Recovery from muscarinic modulation of M current channels requires phosphatidylinositol 4,5-bisphosphate synthesis. *Neuron* **35**, 507–520.

Surprenant A, Rassendren F, Kawashima E, North RA & Buell G (1996). The cytolytic P2Z receptor for extracellular ATP identified as a P2X receptor (P2X7). *Science* **272**, 735–738.

Toker A (1998). The synthesis and cellular roles of phosphatidylinositol 4,5-bisphosphate. *Curr Opin Cell Biol* **10**, 254–261.

Valera S, Hussy N, Evans RJ, Adami N, North RA, Surprenant A & Buell G (1994). A new class of ligand-gated ion channel defined by P2x receptor for extracellular ATP. *Nature* **371**, 516–519.

Vanhaesebroeck B, Leevers SJ, Ahmadi K, Timms J, Katso R, Driscoll PC, Woscholski R, Parker PJ & Waterfield MD (2001). Synthesis and function of 3-phosphorylated inositol lipids. *Annu Rev Biochem* **70**, 535–602.

Virginio C, MacKenzie A, Rassendren FA, North RA & Surprenant A (1999). Pore dilation of neuronal P2X receptor channels. *Nat Neurosci* **2**, 315–321.

Weiner OD, Neilsen PO, Prestwich GD, Kirschner MW, Cantley LC & Bourne HR (2002). A PtdInsP (3) - and Rho GTPase-mediated positive feedback loop regulates neutrophil polarity. *Nat Cell Biol* **4**, 509–513.

Werner P, Seward EP, Buell GN & North RA (1996). Domains of P2X receptors involved in desensitization. *Proc Natl Acad Sci U S A* **93**, 15485–15490.

Wu L, Bauer CS, Zhen XG, Xie C & Yang J (2002). Dual regulation of voltage-gated calcium channels by PtdIns (4,5), P2. *Nature* **419**, 947–952.

Zhainazarov AB, Spehr M, Wetzel CH, Hatt H & Ache BW (2004). Modulation of the olfactory CNG channel by Ptdlns (3,4,5), P3. *J Membr Biol* **201**, 51–57.

Zhang H, Craciun LC, Mirshahi T, Rohacs T, Lopes CM, Jin T & Logothetis DE (2003). PIP (2) activates KCNQ channels, and its hydrolysis underlies receptor-mediated inhibition of M currents. *Neuron* **37**, 963–975.

Zhou Z & Hume RI (1998). Two mechanisms for inward rectification of current flow through the purinoceptor P2X2 class of ATP-gated channels. *J Physiol* **507**, 353–364.

Zhou Z, Monsma LR & Hume RI (1998). Identification of a site that modifies desensitization of P2X2 receptors. *Biochem Biophys Res Commun* **252**, 541–545.

Acknowledments

We are grateful to Dr D. Julius (University of California, San Francisco) for providing us with $P2X_2$ cDNA. We are also grateful to Dr W. Stühmer (Max-Planck-Institut fur Experimentelle Medizin, Gottingen), Dr S. Nakanishi (University of Kyoto) and Dr T. Kubo (AIST, Tsukuba) for providing us with cDNAs encoding rat $P2X_4$ receptor, substance P receptor and porcine M1 receptor. We would like to thank Dr T. Misaka (University of Tokyo) for instructing us in the biochemistry and fluorescence assay, and for insightful suggestions. We would like to thank members of the Kubo laboratory (National Institute for Physiological Sciences) for helpful discussions and Ms Y. Asai for technical assistance. This work was supported in part by research grants from the Ministry of Education, Science, Sports, Culture, and Technology of Japan, and from the Japan Society for Promotion of Science to Y.K., and by a research fellowship from the Japan Society for Promotion of Science for Young Scientists to Y.F.

Author's present address

Y. Fujiwara: Dan Minor Laboratory, Departments of Biochemistry and Biophysics and Cellular and Molecular Pharmacology, University of California San Francisco, MC 2532, Byers Hall Room 304, 1700 4th Street, San Francisco, CA 94158-2330, USA. Email: yuichiro.fujiwara@ucsf.edu

Supplemental material

The online version of this paper can be accessed at:
DOI: 10.1113/jphysiol.2006.115246
http://jp.physoc.org/cgi/content/full/jphysiol.2006.115246/DC1
and contains supplemental material consisting of two figures as follows.

Supplemental Fig. 1. The relationship between the expression level and channel desensitization
Oocytes showing various levels of $P2X_2$ expression were prepared. Data were recorded as in Fig. 2, and the extent of desensitization was plotted against the peak current amplitude. The broken line indicates the linear regression line of the data ($n = 29$).

Supplemental Fig. 2. Electrophysiological measurement of the G_q-coupled receptor response
A, current traces recorded from an oocyte expressing WT $P2X_2$ and M1 receptors after application of 100 μM ACh. Oocytes were held at −80 mV, and depolarizing step pulses to 30 mV were applied every 1 s. *B*, typical example of the time course of the response to the application of 100 μM ACh. The current amplitudes at the end of the step pulses to 30 mV shown by an arrow in *A* were plotted. The bath solution was a Na^+-based external solution with no Ca^{2+}.

This material can also be found as part of the full-text HTML version available from http://www.blackwell-synergy.com